Coherent optical association of a single molecule

Yichao Yu,* Kenneth Wang, J. D. Hood, Lewis Picard, Jessie T. Zhang,

William Cairncross, Jeremy Hutson, Till Rosenband, and Kang-Kuen Ni†

Department of Chemistry and Chemical Biology,
Harvard University, Cambridge, Massachusetts, 02138, USA
Department of Physics, Harvard University, Cambridge, Massachusetts, 02138, USA and
Harvard-MIT Center for Ultracold Atoms, Cambridge, Massachusetts, 02138, USA
(Dated: October 3, 2020)

We report on coherent association of a single weakly-bound NaCs molecule in an optical tweezer through an optical Raman transition without the use of a Feshbach resonance. Our scheme borrows transition dipole moment while reducing photon scattering by selecting a deeply bound electronic excited intermediate state. Starting from two atoms in their relative motional ground state, we achieve optical transfer efficiency of 50% . The molecule has a (change to 8.8G) zero-field binding energy of 770MHz and lifetime up to 1ms . (center of mass motional state population.) This technique is general without relying on narrow excited state lines or Feshbach resonances and could allow a wider range of molecular species to be assembled atom-by-atom. Yichao, can you update numbers in the abstract? also, can you update affiliations in the author list, Jeremy is Durham and Jon is Purdue

Diverse species of fully quantum controlled ultracold molecules are desired for a wide variety of applications including precision measurements [1], quantum simulations [2], quantum information processing [3, 4], and studies of ultracold chemistry [5–7]. While many innovative approaches demonstrated in the last few years have directly cooled different species of diatomic or polyatomic molecules below 1 mK [8, 9], the coldest and the highest phase-space-density gas to date in an ensemble [10] or as individuals [11] have been achieved through the association of ultracold atoms.

Such ultracold molecular association takes advantage of the much developed cooling and trapping techniques for atoms as a starting point. To overcome the challenges of small wavefunction overlap and the large release of binding energy of converting atoms to deeply-bound molecules, a two-step approach has been established to first associate atom pairs into weakly-bound molecules, and then transfer the molecules from this single internal state to a desired rovibrational and electronic state [12–20]. So far, all of such association processes utilized a magnetic Feshbach scattering resonance and have been applied to bialkali molecules. The only exception is Sr_2 where narrow linewidth excited states are available and optical association can be driven coherently [21, 22]. The requirement of a Feshbach resonance to enhance atom-to-molecule wavefunction overlap or the existence of narrow excited state lines limits the generality of the association technique.

Here, we demonstrate coherent association of an atom pair to a weakly bound molecule using a two-photon optical Raman transfer via an electronic excited state, without the use of a Feshbach resonance nor a narrow excited state, schematically shown in Fig. 1A. The resulting single molecule is in a single internal quantum state and predominately in its motional ground state. Our scheme is based on using a theoretically determined vibrational

state of the electronic excited state $c^3\Sigma^+$ that has the best raman Rabi frequency to photon scattering ratio. To further increase this ratio and reduce technical requirements such as intensity stability, we choose an initial and final state where the matrix elements with the excited state are as balanced as possible. This approach minimizes the reliance on system specific properties and could therefore be applied to creating other molecular species or larger molecules atom-by-atom with full quantum state control.

The essence of an optical Raman transfer can be illustrated using a three-level system (Fig. 1A), where the initial atomic state, the target weakly-bound molecular state are coupled to an excited intermediate state by two photons, Ω_a and Ω_m, with single photon detuning Δ, and two photon detuning, δ. The transfer Raman Rabi Rate is $\Omega_a\Omega_m/2\Delta$ accompanied by a photon scattering rate of $\Gamma_e\Omega/4\Delta^2$...(sum of i termsKW: I was intending to only mention the sum over terms at the end when we exit the 3 level system.)check factor of 2. KW: The 2 in the denominator is including cross coupling. 4 without cross coupling. Since cross coupling is mentioned later, maybe leave this with 4?, where Γ_e is the excited state linewidth [23]. Unlike for Raman transitions in atoms, the two matrix elements here, Ω_m and Ω_a, are greatly imbalanced due to the small wavefunction overlap between the atomic state and the excited molecular state. The scattering rate therefore predominantly comes from the molecular state, $\Gamma_e\Omega_m^2/2\Delta^2$, where Γ_e is the excited state linewidth. (blue text can potentially be moved to footnote) Furthermore, because the energy difference of the atomic and the weakly bound states are small (<1 GHz) comparing to Δ, the power of the Raman beams are chosen to be equal to gives the largest Raman Rabi rate at a fixed total power. An additional factor of 2 is included in the scattering rate because the molecular state scatters off of both Raman beams at roughly the same single
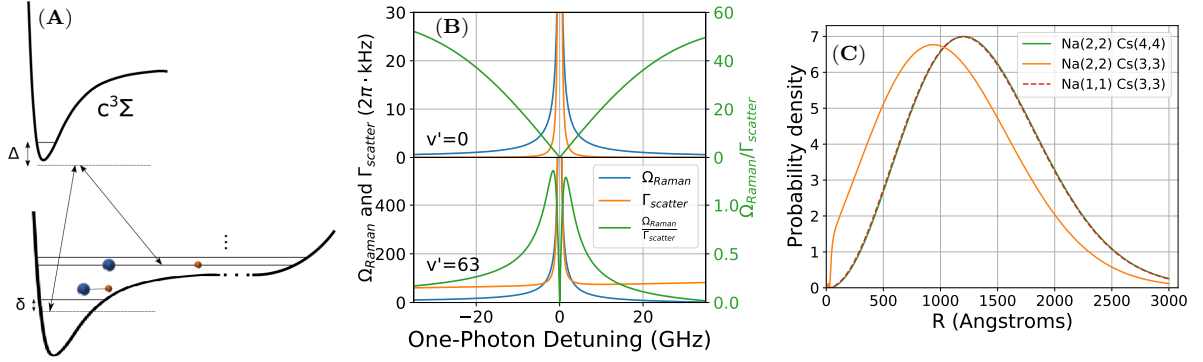
FIG. 1. Optical creation of single molecule from single atoms in tweezer. (A) Schematics of the optical transition from an atom pair to a weakly bound molecule. The initial state is the relative motional ground state between the two atoms and the final state is the first molecular bound state. The transition is driven by a pair of laser frequencies matching the binding energy of the molecule. The lasers are detuned from an excited molecular state in the $c^3\Sigma$ potential by Δ in order to suppress the scattering during the transfer. (B) Comparison between using a weakly bound and a deeply bound excited state as intermediate state for the Raman transition. The deeply bound excited state (upper half $v = 0$) has a smaller Raman Rabi frequency (Ω_{Raman}) compared to the weakly bound excited state (lower half $v = 63$) at a given detuning. However, the scattering rate ($\Gamma_{scatter}$) is also much lower, which results in a larger Raman Rabi frequency to scattering rate ratio. (C) Enhancement of short range wavefunction. The large scattering length for the $Na(2,2), Cs(3,3)$ state creates an interaction shift comparable to the axial trapping frequency. This causes a significant change in the relative wavefunction especially at short intranuclear distance (R). Compared to other spin states with weaker interaction, the wavefunction at short distance ($R < 100$Å) is significantly enhanced.

photon detuning. Thus, the ratio between the Raman Rabi frequency and the scattering rate, $\Omega_a/\Omega_m \times \Delta/\Gamma_e$, depends on the ratio of the two matrix elements and how far detuned the laser is from the transition in units of the linewidth. To ensure a coherent process, larger detuning is preferred while achieving a realistic Raman Rabi frequency. With the multiple excited vibrational states present in a molecular potential, the total scattering rates and Rabi rates become a sum of the scattering rates and Rabi rates over all the states.

Pioneering experiments used weakly bound molecular excited states in the Raman transition to ensure a large Raman Rabi frequency [24, 25]. However, such choice of state suffers from strong scattering of the nearby atomic excited state to render it incoherent, resulting in molecule loss. The scattering is proportional to $1/\delta_{thresh}^2$, where δ_{thresh} is the detuning from the dissociation threshold, and thus can be made smaller by detuning away from the dissociation threshold.

To find the optimal excited intermediate state, we perform a calculation of the Raman Rabi frequency and scattering rate at different detunings from the atomic threshold taking into account of all states of the $c^3\Sigma$ excited molecular state potential (full result in SM) [26] KW: I have only done the calculations with c3Sigma only, cause the b3Pi is highly spin orbit coupled, and not necessarily trustworthy where we are. I can also include a citation to the paper with that potential?. As shown in Fig. 1B, the ratio of the Raman Rabi rate to scattering rate can be made larger for more deeply bound states compared to weakly bound states at a cost of a smaller Raman Rabi

frequency. As a result, we choose a deeply bound molecular excited state ($v' = 0$ of $c^3\Sigma^+$) as an intermediate state to drive the Raman transition.

Main point here. Small Ω_a/Ω_m ratio can be compensated by larger detuning, but Stark shift is problematic. KW: I agree Stark shift limitation is definitely pretty problematic, but I would also argue that larger detuning may not be able to save the day, because of the many vibrational states in a molecular potential, the lower Raman rabi frequency which results from detuning farther and possibly running into other limitations if you have to do that, such as the background off resonant scattering rate from near threshold states or technical background scattering. yes, I agree. I want to layout the structure .... motivate for the better ratio first, than talk about choosing the state. KW: Okay, got it. Makes sense. In addition to the intermediate state, the choice of the initial and final states is also critical. As previously discussed, the ratio of the Raman Rabi rate to the scattering rate is proportional to the Ω_a/Ω_m ratio. The smaller this ratio is, the farther the laser needs to be detuned to achieve the same Raman Rabi rate to scattering rate ratio, which lowers the Raman Rabi rate. This ratio can be made larger by increasing the coupling of the atomic state with the excited molecular state. Due to the small size of the molecular wavefunction, the coupling between the ground atomic state and the excited molecular state is approximately proportional to the value of the relative atomic wavefunction at short distance within the molecular potential. In addition to the confinement, this value is related to the interaction between the two

atoms. For states with a large scattering length (positive or negative), the phase shift in the relative wavefunction between the atoms can significantly increase the short range wavefunction (Fig. 1C). The increase in the coupling is proportional to (quote/cite Olive's equation?). For our system, among the stable spin combinations, 4422 and 3311 both have small scattering lengths of $a_{4422} = 30.4a_0, a_{3311} = 13.7a_0$ respectively, but the 3332 combination has a large and negative scattering length of $a_{3322} = -693.8a_0$ (interaction shift ≈ binding?) [27]. In addition to the increased atomic coupling, Ω_a, with the 3322 hyperfine combination, coupled channel calculations show that the most weakly bound molecular state that is predominantly in the 3322 spin combination also has reduced coupling, Ω_m, with the excited state when compared with the 4422 and 3311 bound states. Therefore, using an initial 3322 hyperfine combination results in a Ω_a/Ω_m ratio of about 0.05 instead of a ratio of about 0.003 with the 4422 or 3311 combinations. In addition to reducing how far the laser needs to be detuned from the transition, a larger Ω_a/Ω_m ratio also relaxes the intensity stability requirement, a key potential technical limitation. The position of the resonance depends on the laser power predominantly through the AC Stark shift on the molecular state, $\Omega_m^2/2\Delta$. KW: Can also include similar footnote here about cross coupling? The 2 in the denominator is assuming cross coupling and equal powers. The ratio of the AC Stark shift to the Raman Rabi frequency is Ω_m/Ω_a, Thus, the laser intensity needs to be stabilized to better than the inverse of this ratio to fluctuate by less than a linewidth in a coherent process. Thus, instead of a required intensity stability of 0.3% for the 4422 or 3311 combination, the 3322 combination only requires the intensity to be stabilized to 5%. Thus, we choose the 3322 spin combination as our initial state and drive to the first bound state for the 3322 spin combination. (We might want to mention that those ratios are for 80 kHz spherical trap if we want to give more details about the coupled channel calculation anywhere...)

To perform the Raman transfer, we use our apparatus described in our previous work [28]. Our experiment begins by stochastically loading a single ^{23}Na atom and a single ^{133}Cs atom into an optical tweezer from a dual-species MOT into separate optical tweezers. The atoms are initially imaged to distinguish between loading of two atoms, one atom (Na or Cs), or no atom in order to perform post selection. We then perform simultaneous Raman sideband cooling (RSC) to cool both atoms into the 3-dimensional motional ground state of their optical tweezers. After RSC, the Na tweezer is moved by sweeping the frequency on an acoustical optical beam deflector (AOBD) to overlap with the Cs tweezer before smoothly ramping off, so that the Na and Cs atoms are merged into the same tweezer [28]. The spin states for the Na and Cs atoms after RSC and during the merge process are $|F = 2, m_F = 2\rangle_{Na}$ and $|F = 4, m_F = 4\rangle_{Cs}$ re-

spectively. This states combination has a low scattering length, which allows the two atoms to be merged into the same tweezer with minimum pertubation on each other and thus they remain in the motional ground state after the merge.

After preparing the Na and Cs atoms in the same tweezer in a single quantum state, we need to drive the atoms into the large scattering length 3322 hyperfine combination. To do this, we perform a spin flip taking into account the interaction shift [27] using a Cs Raman transition to drive the Cs atom into the $|F = 3, m_F = 3\rangle_{Cs}$ state. The new spin state combination has a larger scattering length of $-693.8a_0$ which generates a interaction shift of $-30.7kHz$ in the tweezer. This interaction shift is larger than the differential axial trapping frequency between Na and Cs atoms, which decouples the relative and center of mass motional state and improves the robustness of our preparation of the relative motion ground state.

After the atoms are prepared in the 3322 hyperfine combination, we then perform the Raman transfer. The pulse sequence for this step is shown in Fig. 2B. Instead of adding another beam to drive the Raman transition on the atoms in the tweezer, we use the tweezer itself to achieve this goal. In particular, we turn on two co-propagating frequencies in the tweezer during the Raman pulse. The dual use of the tweezer beam ensures that there is not any undesired laser frequency that can interfere with the Raman transition, and also allows us to maximize the Raman Rabi frequency and minimize the transfer time. After the total tweezer power is set to the desired value, we smoothly ramp down the power of one frequency in the tweezer while simultaneously ramping up the power of a different frequency so that the total tweezer power remains unchanged. Both frequencies are kept on for a variable length of time before the process is reversed and we return to having a single frequency in the tweezer. In additional to reducing the number of laser beams during the Raman transition, we also found the spectral purity of the laser to be critical for achieving a higher transfer efficiency. The tweezer and Raman beams are generated by amplifying a 1037nm external cavity diode laser (ECDL) with a Raman fiber amplifier, which produces a broad band amplified spontaneous emission (ASE), in addtional to the desired frequency, and increases the scattering rate due to coupline to other excited states. We use a bragg grating with a line width (FWHM) of 50GHz to clean up the laser spectrum and found it reduces the scattering rate by at least a factor of 2 for certain tweezer detuning.

Guided by coupled channel calculations, we locate the Raman resonance for the atom to molecule transition at 770.59430(17)MHz (Fig. 2C) with a $15mW$ tweezer at $288560GHz$ which corresponds to a $145GHz$ single photon detuning. (We can maybe add information about the prediction here?) The background level of 31% cor-
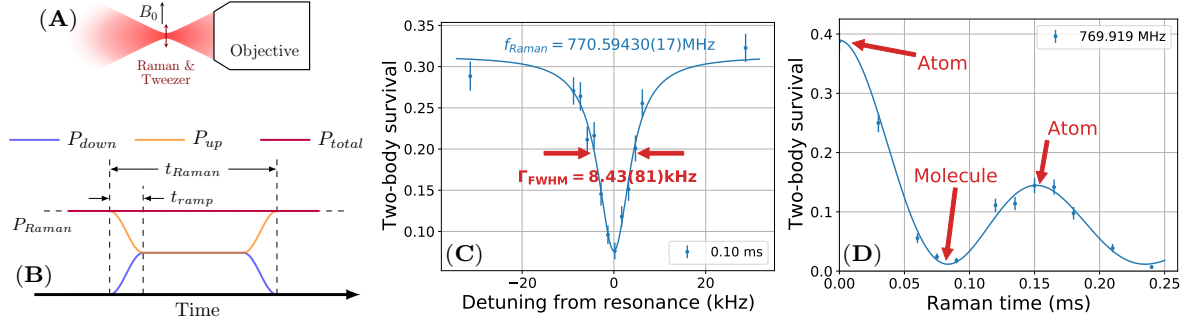
FIG. 2. (A) Geometry and polarization of trap and Raman beam relative to the bias magnetic field. The tweezer and Raman beam is focused through an objective to define the location of the atoms and molecule. We use a bias B field of $B_0 = 8.8G$ alone the tweezer polarization to define the quantization axis. As a result, the atoms experiences predominately π polarization from the tweezer. (B) Molecule formation pulse sequence. The tweezer initially consists of only up leg power. When driving the Raman transition, the up leg power is smoothly ramped down and the down leg power ramped up over $10\mu s$ while maintaining the total power of the tweezer. This minimizes the heating on the atoms due to power fluctuation while maximizes the time with maximum Raman Rabi frequency when the up and down leg powers are equal. (C) Raman resonance from atomic state $Na(2,2)\, Cs(3,3)$ to the first molecular bound state using a 0.1ms pulse. The full width half maximum (FWHM) of 8.43(81)kHz of the resonance is consistent with the FWHM for a coherent 0.1ms 8.0kHz π pulse. (D) Raman pulse time scan on resonance. A decaying Rabi oscillation can be observed proving the coherence of the Raman transfer process.

responds to the probability of preparing the two atoms in the relative motional ground state. When the atoms are transferred into the molecule state by the Raman transition, there is a decrease in the two body survival since the resulting molecule is not directly detected by our imaging step. We observed the narrowest linewidth of 8.43(81)kHz for the Raman resonance at a pulse time of 0.1ms, which corresponds to a linewidth-pulsetime product of 0.843(81). This is consistent with the expected value of 0.80 for an ideal π pulse which is an evidence that the transfer is coherent. In order to verify the coherence of the transfer directly, we fix the Raman frequency on resonance and scan the pulse time. Fig. 2D shows the observed Rabi oscillation between the atomic and molecular states. Fitting the data with a decaying Rabi oscillation suggests that 63% of initial ground state atoms are transferred into the molecular state.

In order to understand the fidelity of molecule formation, we fit our measurements to a model that includes a Raman Rabi frequency and a finite lifetime for the final molecular state (Fig. 3A). We account for the effect of atomic state loss by measuring the single and two body lifetime of the atoms directly (Fig. 3B). The fit shows that we have a Raman Rabi frequency of .... The molecule we form has a lifetime of $84.9(49)\mu s$ which is the main limitation on the fidelity of the transfer. The molecule lifetime can be verified directly by adding a second Raman pulse to dissociate the molecule back to atoms after a variable wait time (Fig. 3C). The result shows a molecular lifetime consistent with our fitting of the decaying Rabi oscillation.

The ratio of molecule scattering rate to the Rabi frequency is larger than the theory prediction. In order to understand the origin of this discrepancy, we measured the dependency of the Raman resonance (what does dependence of the Raman resonance mean? Do you just mean we measured molecule formation as a function of all these parameters?) as a function of the tweezer power and single photon frequency. The important results from the fits are the 2 photon resonance frequency (light shift), Raman Rabi frequency, atomic lifetime and molecular lifetime. Each of these quantities provide us with information about a different combination of physical processes.

First we look at the change in resonance frequency. As a function of the tweezer power, we observe a linear dependency on the resonance frequency caused by the differential light shift between the atomic and molecular state (Fig. 4A). When we vary the tweezer frequency around the $v = 0$ excited state, we can further observe a $1/\delta$ component and a background component that is constant for different detunings in the experimentally explored region. The background is caused by coupling to other excited states that are further away in energy. The $1/\delta$ component, however, is predominantly due to the coupling between the molecular state and the $v = 0$ excited state. From this measurement, we can calculate a matrix element between the molecular state and the excited state, Ω_m, of .... which is similar to what we calculated from theory (ref/sm theory). (make sure theory part mentions $\Omega_{down} \gg \Omega_{up}$, also Ω vs Ω' for the single leg vs cross coupling number).

(talk about blue side?)

Next, we discuss the dependencies of the Raman Rabi frequency. The Raman Rabi frequency shows a nonlinear dependency on the tweezer power due to the
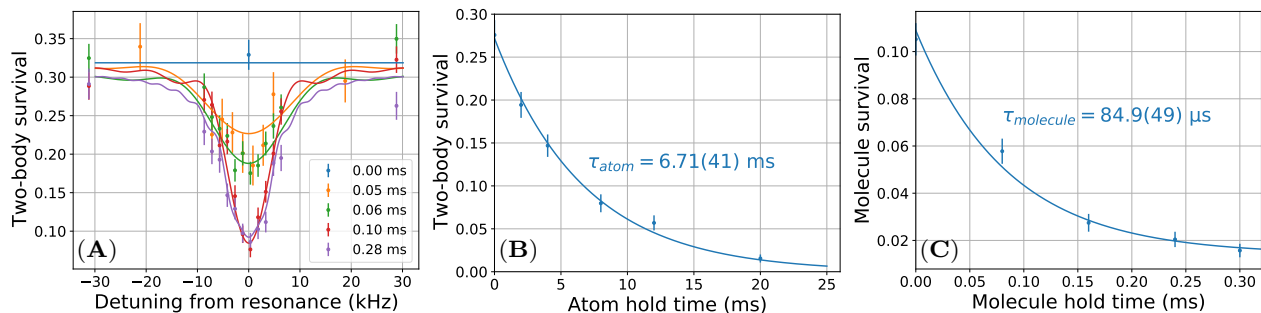
FIG. 3. (A) Fitting of Raman detuning scans at different times to a model of Raman transition with loss on the atom and molecule state. The combined fit is used to determine both the Raman Rabi frequency and the loss rates. (B) Two-body atom lifetime in 15mW of trap depth caused by off-resonance photoassociation. This is used to improve the fitting of the Raman transfer data. (C) Direct measurement of molecule lifetime in 15mW of trap depth. Molecule survival is detected by dissociating back to atoms using a second Raman transition. The lifetime is consistent with the $84.9(49)\mu s$ measured from the Raman transition data.

change in the atomic wavefunction caused by the change in confinement (Fig. 4?). The atomic matrix element, Ω_a, is proportional to the the short range atomic wavefunction amplitude, which scales as $P^{0.375}$ for weakly interacting particles. However, due to the strong interaction between the two atoms, this approximation breaks down. Instead, theory calculation shows that the scaling is very well approximated by $P^{0.29}$ within the range of confinement in our experiment. Combined with the intensity factor, the Raman Rabi frequency should scale with $P^{1.29}$, which agrees with our experimental result. Similar to the light shift, there is also a background component and a $v = 0$ component in the Raman Rabi frequency. The $v = 0$ component predicts a up leg Rabi frequency of ... which is consistent with theory. Unfortunately, the background Raman Rabi frequency cancels the Rabi frequency for red detuning Raman transition which is one of the factors that decreases our transfer efficiency. (need blue side?)

Next, we look at the atomic loss rate during the transfer process. (Fig. 4?) The atomic loss rate scales as $P^{2.58}$ but shows little to no dependency on the tweezer frequency. The lack of frequency dependency suggests that most of the atomic loss are due to the coupling to states other than $v = 0$. After subtracting 0.58 from the power scaling due to the effect of confinement on the square of the atomic matrix element, the loss rate is proportional to P^2. This is evidence that the loss is likely caused by a two photon scattering process rather than one photon scattering. The strong power scaling causes a faster than expected loss rate for the atom. However, the atomic scattering rate contributes only a small fraction of the total scattering rate so this is not the limiting factor for the transfer.

Finally, we fit the scaling for the molecular loss rate. (Fig. 4?) We observed a dependency on the detuning that is consistent with $1/\delta^2$ suggesting that the loss is indeed

mostly coming from the $v = 0$ excited state (but this is only true at certain single photon detunings?). (preliminary) We observed a power scaling power of ≈ 1.2 which is closed to the prediction for a single photon scattering process. The excited state line width calculated from the scattering rate is ...$(1GHz?)$ which is much larger than the theory prediction of $10MHz$ as well as the $20MHz$ upper bound from our previous PA measurements (cite).

B field dependency ...kHz/G which agrees with theory prediction of ...kHz/G. Dependency on tweezer power ...kHz/mW, extrapolated to obtain the bare resonance at 0 tweezer power to be at ...MHz.

---

* yichaoyu@g.harvard.edu
† ni@chemistry.harvard.edu

[1] I. Kozyryev and N. R. Hutzler, Physical Review Letters **119**, 133002 (2017), publisher: American Physical Society.

[2] N. Y. Yao, M. P. Zaletel, D. M. Stamper-Kurn, and A. Vishwanath, Nature Physics **14**, 405 (2018).

[3] D. DeMille, Phys. Rev. Lett. **88**, 067901 (2002).

[4] K.-K. Ni, T. Rosenband, and D. D. Grimes, Chem. Sci. **9**, 6830 (2018).

[5] J. L. Bohn, A. M. Rey, and J. Ye, Science **357**, 1002 (2017).

[6] N. Balakrishnan, J. Chem. Phys. **145**, 150901 (2016), http://dx.doi.org/10.1063/1.4964096.

[7] M.-G. Hu, Y. Liu, D. D. Grimes, Y.-W. Lin, A. H. Gheorghe, R. Vexiau, N. Bouloufa-Maafa, O. Dulieu, T. Rosenband, and K.-K. Ni, Science **366**, 1111 (2019), https://science.sciencemag.org/content/366/6469/1111.full.pdf.

[8] E. B. Norrgard, D. J. McCarron, M. H. Steinecker, M. R. Tarbutt, and D. DeMille, Phys. Rev. Lett. **116**, 063004 (2016).

[9] D. Mitra, N. B. Vilas, C. Hallas, L. Anderegg, B. L. Augenbraun, L. Baum, C. Miller, S. Raval, and J. M. Doyle, Science **369**, 1366 (2020),
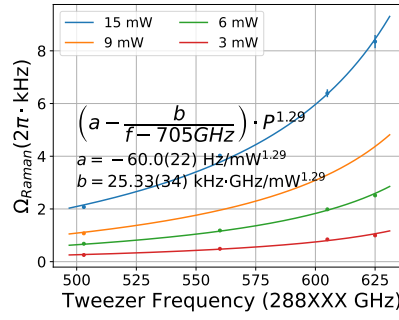
FIG. 4. Raman transition parameters as a function of tweezer/Raman power and detuning. (A) Raman Rabi frequency scales as $P_{tweezer}^{1.29}$ and follows $1/\delta$ with an offset. (B) Atom loss rate scales as $P_{tweezer}^{2.58}$ suggesting a two-photon scattering loss. (C) Molecular loss rate scales closed to $P_{tweezer}$ and follows $1/\delta^2$ with additional detuning independent background loss rate. This result controdicts the our previous measurement of excited state lifetime suggesting that there are additional loss mechanism that is not taken into account.

https://science.sciencemag.org/content/369/6509/1366.full.pdf.

[10] L. De Marco, G. Valtolina, K. Matsuda, W. G. Tobias, J. P. Covey, and J. Ye, arXiv preprint arXiv:1808.00028 (2018).

[11] J. T. Zhang, Y. Yu, W. B. Cairncross, K. Wang, L. R. B. Picard, J. D. Hood, Y.-W. Lin, J. M. Hutson, and K.-K. Ni, Phys. Rev. Lett. 124, 253401 (2020).

[12] J. G. Danzl, E. Haller, M. Gustavsson, M. J. Mark, R. Hart, N. Bouloufa, O. Dulieu, H. Ritsch, and H.-C. Nägerl, Science 321, 1062 (2008).

[13] K.-K. Ni, S. Ospelkaus, M. H. G. de Miranda, A. Pe'er, B. Neyenhuis, J. J. Zirbel, S. Kotochigova, P. S. Julienne, D. S. Jin, and J. Ye, Science 322, 231 (2008).

[14] F. Lang, K. Winkler, C. Strauss, R. Grimm, and J. Hecker Denschlag, Phys. Rev. Lett. 101, 133005 (2008).

[15] T. Takekoshi, L. Reichsöllner, A. Schindewolf, J. M. Hutson, C. R. Le Sueur, O. Dulieu, F. Ferlaino, R. Grimm, and H.-C. Nägerl, Phys. Rev. Lett. 113, 205301 (2014).

[16] P. K. Molony, P. D. Gregory, Z. Ji, B. Lu, M. P. Köppinger, C. R. Le Sueur, C. L. Blackley, J. M. Hutson, and S. L. Cornish, Phys. Rev. Lett. 113, 255301 (2014).

[17] J. W. Park, S. A. Will, and M. W. Zwierlein, Phys. Rev. Lett. 114, 205302 (2015).

[18] M. Guo, B. Zhu, B. Lu, X. Ye, F. Wang, R. Vexiau, N. Bouloufa-Maafa, G. Quéméner, O. Dulieu, and D. Wang, Phys. Rev. Lett. 116, 205303 (2016).

[19] S. S. Kondov, C.-H. Lee, K. H. Leung, C. Liedl, I. Majewska, R. Moszynski, and T. Zelevinsky, Nature Physics 15, 1118–1122 (2019).

[20] K. K. Voges, P. Gersema, M. Meyer zum Alten Borgloh, T. A. Schulze, T. Hartmann, A. Zenesini, and S. Ospelkaus, Phys. Rev. Lett. 125, 083401 (2020).

[21] G. Reinaudi, C. B. Osborn, M. McDonald, S. Kotochigova, and T. Zelevinsky, Phys. Rev. Lett. 109, 115303 (2012).

[22] S. Stellmer, B. Pasquiou, R. Grimm, and F. Schreck, Phys. Rev. Lett. 109, 115302 (2012).

[23] D. J. Wineland, M. Barrett, J. Britton, J. Chiaverini, B. DeMarco, W. M. Itano, B. Jelenković, C. Langer, D. Leibfried, V. Meyer, T. Rosenband, and T. Schätz, Philosophical Transactions of the Royal Society of London A: Mathematical, Physical and Engineering Sciences 361, 1349 (2003), http://rsta.royalsocietypublishing.org/content/361/1808/1349.full.pdf.

[24] R. Wynar, R. S. Freeland, D. J. Han, C. Ryu, and D. J. Heinzen, Science 287, 1016 (2000), http://science.sciencemag.org/content/287/5455/1016.full.pdf.

[25] T. Rom, T. Best, O. Mandel, A. Widera, M. Greiner, T. W. Hänsch, and I. Bloch, Phys. Rev. Lett. 93, 073002 (2004).

[26] L. R. Liu, J. T. Zhang, Y. Yu, N. R. Hutzler, Y. Liu, T. Rosenband, and K.-K. Ni, arXiv:1701.03121 .

[27] J. D. Hood, Y. Yu, Y.-W. Lin, J. T. Zhang, K. Wang, L. R. Liu, B. Gao, and K.-K. Ni, Phys. Rev. Research 2, 023108 (2020).

[28] L. R. Liu, J. D. Hood, Y. Yu, J. T. Zhang, K. Wang, Y.-W. Lin, T. Rosenband, and K.-K. Ni, Phys. Rev. X 9, 021039 (2019).